Aircraft Landing-Induced Tire Spinup

Joe Padovan*
University of Akron, Akron, Ohio 44325
Amir Kazempour†
Goodyear Tire and Rubber Company, Akron, Ohio 44316
and
Yong Hee Kim‡
University of Akron, Akron, Ohio 44325

Based on the appropriate stiffness and inertial properties of prototypical aircraft landing gear suspension systems, a tire spinup model is developed. Because of its generality, the model can define the various governing dynamical fields. Here, the effects of such factors as sink rate, runway friction, and aircraft landing speed are considered. Main attention is given to defining the tire deflection-rotation-skidding history as well as the net and pointwise rate of work due to interfacial friction as it effects the growth of rotary inertia and slip work. To quantify the influence of such factors as sink rate, friction, and landing speed, a case study involving the Shuttle main tires is included.

Nomenclature

a_2, a_3	= curving fitting parameters
C_S	= suspension damping
C_T	= tire damping
F_M	= tire friction force
F_N	= normal tire force
g	= gravitational constant
J_T	= tire polar moment of inertia
K_S	= suspension stiffness
K_T	= tire lateral stiffness (linear)
KE	= kinetic energy
${}_H(\mathrm{KE})_A$	= horizontal vehicle KE
${}_R(\mathrm{KE})_T$	= tire rotary KE
${}_TK_T$	= torsional tire stiffness
L_c	= length of contact patch
M_A	= mass of aircraft
M_a	= mass of tire-axle-brake-wheel pair
P_I	= internal tire pressure
R	= tire radius
S_D	= skid distance
t_E	= end of spinup
t_I	= initiation of spinup
t_R	= residency time, $=(t_E-t_I)$
U	= deformation
V_L	= landing velocity
V_{slip}	= slip velocity
V_{SR}	= sink rate
W_{slip}	= slip work
Δt_R	= time step
δ_a	= axle displacement
δ_A	= aircraft displacement
ρ	= density
μ	= friction coefficient
θ	= angular position
$\otimes$	= cross product

Received April 17, 1990; revision received Aug. 13, 1990; accepted for publication Aug. 13, 1990. Copyright © 1990 by the American Institute of Aeronautics and Astronautics, Inc. All rights reserved.

*Department of Mechanical Engineering.
†Engineer.
‡Graduate Student, Department of Mechanical Engineering.

I. Introduction

BECAUSE of weight limitations, traditional aircraft landing systems do not provide for tire spinup prior to touchdown.[1] For lightweight aircraft with low approach velocities, the touchdown-induced spinup process does not represent a problem. This is clearly demonstrated in recent wear studies funded by the Air Force[2] as well as in the comprehensive design handbook on landing gear of Currey.[1] This latter work provides an overview of the pertinent literature on the subject.

On the other end of the scale, the NASA Space Shuttle tires undergo significant wear during landing.[3,4] This is a direct result of the runway conditions and the spinup inertias induced by the very high approach velocity required to prevent stalling. Such problems point to potential wear difficulties in all high speed landings. In this context, it is desirable to develop a better understanding of the parametric sensitivities associated with the spinup problem. To this end, the current paper develops an analytical model that defines the transient response generated during landing.

Overall, the model incorporates the stiffness and inertial properties of the suspension and tire along with the effects of such factors as sink rate, runway friction, and vehicle landing velocity. Special attention is given to defining the deflection, rotation-sliding histories, as well as the net and pointwise growth of rotary kinetic energy and slip work due to interfacial friction. These capabilities will enable us to establish such response characteristics as 1) skidding distance, 2) slip (friction) work as a function of tire periphery position, and 3) rate of spinup. In the sections which follow, detailed discussions are given on model development, solution procedure, and a case study involving the Shuttle main tires.

II. Model Development

The modeling of the tire spinup problem associated with aircraft landings requires the characterization of several contributing factors: 1) tire-runway interface, 2) tire-axle characteristics, and 3) axle-suspension-aircraft connection.

Considering the tire runway interface, the principal mode of energy interchange is associated with the friction load induced by the sliding interface. In particular, the work associated with friction falls into two categories, namely 1) that which induces the rotary kinetic energy (KE) change in the tire and 2) that associated with interfacial heat buildup and wear of the tire and runway surfaces.

Such energy interchanges are balanced by a reduction in the horizontal kinetic energy of the aircraft ${}_H(\mathrm{KE})_A$. The global free body diagram of the landing process is illustrated in Fig. 1. While landing, the interplay among the lift, drag, and gravity forces are controlled by pilot interactions. Because of this, the small change in ${}_H(\mathrm{KE})_A$ induced during spinup is caused by the tire-runway interfacial friction force. During such an instant, it follows that

$$\frac{\mathrm{d}}{\mathrm{d}t}\left\{{}_H(\mathrm{KE})_A\right\} = F_\mu(t)V_L(t) \tag{1}$$

or, in integral form, we have

$$\int_0^t \frac{\mathrm{d}}{\mathrm{d}t}\left\{{}_H(\mathrm{KE})_A\right\}\mathrm{d}\tau = \int_0^t F_\mu(\tau)V_L\,\mathrm{d}\tau \tag{2}$$

Noting Fig. 2, the instantaneous velocity of a point on the tire periphery is given by the expression

$$V_{TP} = \frac{\mathrm{d}}{\mathrm{d}t}(R + U) \tag{3}$$

such that R defines the undeformed position of a particle and U is deformation. From a lumped parameter point of view, V_{TP} can be approximated by the expression

$$V_{TP}(t) \sim [R(0) - \delta_a(t)]\frac{\mathrm{d}}{\mathrm{d}t}[\theta(t)] \tag{4}$$

Based on Eq. (3), the three-dimensional rotary conservation of energy equation associated with the tire takes the form[5]

$$\int_{\partial R} F_\mu \otimes \frac{\mathrm{d}}{\mathrm{d}t}(R + U)\,\mathrm{d}s = \int_R \rho(R + U) \otimes \frac{\mathrm{d}}{\mathrm{d}t}(R + U)\,\mathrm{d}v \tag{5}$$

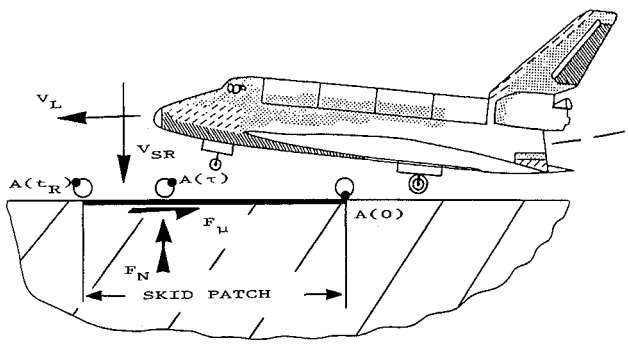

Fig. 1 Free-body diagram of aircraft during landing—tire spinup process.

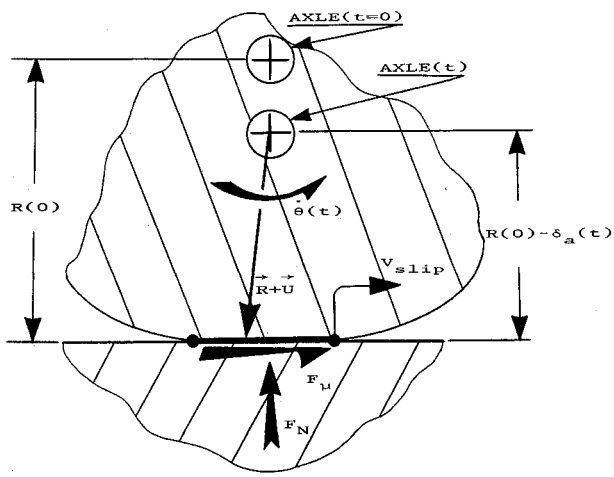

Fig. 2 Periphery velocity of tire.

such that ( ) ⊗ ( ) defines the cross product. Reduced to a lump parameter format, Eq. (5) yields the expression

$$F_\mu(t)[R(0) - \delta_a(t)]\frac{\mathrm{d}}{\mathrm{d}t}[\theta(t)] \sim J_T\frac{\mathrm{d}}{\mathrm{d}t}(\theta)\frac{\mathrm{d}^2}{\mathrm{d}t^2}(\theta) \tag{6}$$

such that J_T is the net polar moment of inertia of the tire-brake-axle system. Since the tire's rotary KE is given by the relation

$${}_R(\mathrm{KE})_T \sim \frac{1}{2}J_T\left(\frac{\mathrm{d}}{\mathrm{d}t}(\theta)\right)^2 \tag{7}$$

we see that

$$F_\mu(t)[R(0) - \delta_a(t)]\frac{\mathrm{d}}{\mathrm{d}t}[\theta(t)] \sim \frac{\mathrm{d}}{\mathrm{d}t}\left\{{}_R(\mathrm{KE})_T\right\} \tag{8}$$

The work associated with wear and heat buildup, i.e., slip work, can be cast in the form

$$\frac{\mathrm{d}}{\mathrm{d}t}(W_{\mathrm{slip}}) = F_\mu V_{\mathrm{slip}} \tag{9}$$

In terms of Eq. (3), the pointwise slip velocity in the contact region is

$$V_{\mathrm{slip}} = V_L - \frac{\mathrm{d}}{\mathrm{d}t}(R + U) \tag{10}$$

or, from a lumped point of view,

$$V_{\mathrm{slip}} \sim V_L - [(R(0) - \delta_a(t)]\frac{\mathrm{d}}{\mathrm{d}t}(\theta)(t) \tag{11}$$

To obtain the net balance of the flow of energies, sum the rate of growth of the tire's rotary kinetic energy ${}_R(\mathrm{KE})_T$ and the slip work W_{slip} to yield the following differential (rate) and integral expressions,

Rate:

$$\frac{\mathrm{d}}{\mathrm{d}t}\left\{{}_H(\mathrm{KE})_A\right\} = \frac{\mathrm{d}}{\mathrm{d}t}\left\{{}_R(\mathrm{KE})_T\right\} + F_\mu V_{\mathrm{slip}} \tag{12}$$

Integral:

$$\int_o^t \frac{\mathrm{d}}{\mathrm{d}t}\left\{{}_H(\mathrm{KE})_A\right\}\mathrm{d}t = \int_o^t \frac{\mathrm{d}}{\mathrm{d}t}\left\{{}_R(\mathrm{KE})_T\right\}\mathrm{d}t + \int_o^t F_\mu(\tau)V_{\mathrm{slip}}(\tau)\,\mathrm{d}\tau \tag{13}$$

Assuming a Columb type friction law,[6] it follows that

$$F_\mu = \mu F_N \tag{14}$$

where typically $0 < \mu < 1$. Noting Fig. 3, the normal force F_N is dependent on the vertical characteristics of the tire suspension system. From a lumped point of view, depending on the tire internal pressure P_I, the axle load deflection curve displays hardening-type nonlinear behavior.[7] This is illustrated by the experimental data[8] given in Fig. 4. Here, it follows that

$$F_N = K_T\sigma_a + a_2\sigma_a^2 + a_3\sigma_a^3 \tag{15}$$

Based on Eq. (15), the governing vertical tire-suspension-aircraft equations take the form

$$M_a\frac{\mathrm{d}^2}{\mathrm{d}t^2}(\delta_a) + [C_T + C_S(\delta_a, \delta_A)]\frac{\mathrm{d}}{\mathrm{d}t}(\delta_a) + (K_T + K_s)\delta_a + a_2\delta_a^2 + a_3\delta_a^3 = C_S(\delta_a, \delta_A)\frac{\mathrm{d}}{\mathrm{d}t}(\delta_A) + K_S\delta_A \tag{16}$$

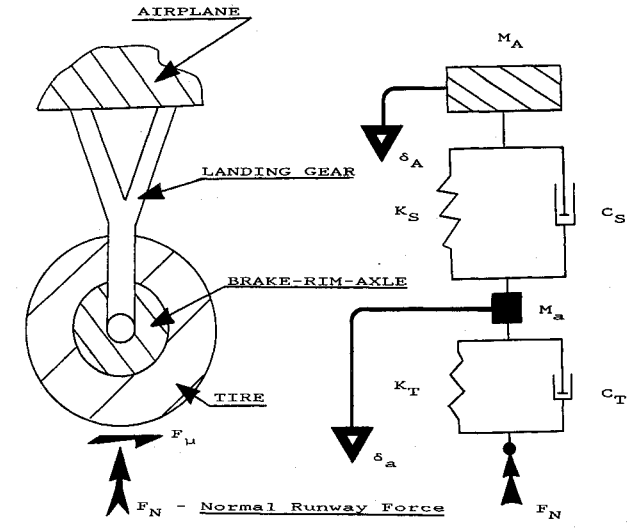

Fig. 3 Vertical suspension model.

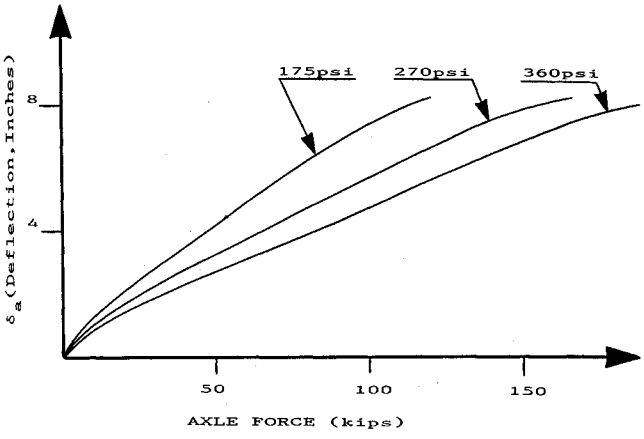

Fig. 4 Axle force-deflection characteristics: the Shuttle main tire.

$$M_A \frac{d^2}{dt^2}(\delta_A) + C_S(\delta_a, \delta_A)\frac{d}{dt}(\delta_A) + K_S\delta_A = K_s\delta_a + C_S(\delta_a, \delta_A)\frac{d}{dt}(\delta_a) \tag{17}$$

Recall that pilot interaction balances lift, drag, and weight leading to a sink rate V_{SR} along the landing approach trajectory. This yields the following initial conditions for Eqs. (16) and (17), namely at $t = 0$

$$\delta_A(0) = \delta_a(0) = 0 \tag{18a}$$

$$\frac{d}{dt}[\delta_A(0)] = \frac{d}{dt}[\delta_a(0)] = V_{SR} \tag{18b}$$

To complete the equations, if the tires potential twist up due to torque loading is admitted, then Eq. (6) takes the form

$$J_T \frac{d^2}{dt^2}(\theta) + {}_TK_T\,\theta = F_\mu(R - \delta_a) \tag{19}$$

Based on Eq. (19), we see that

$$\frac{d}{dt}\left\{{}_H(\mathrm{KE})_A\right\} = \frac{d}{dt}\left\{{}_R(\mathrm{KE})_T\right\} + {}_TK_T\,\theta + F_\mu V_{\text{slip}} \tag{20}$$

The initial conditions associated with Eq. (20) are given by

$$\theta(0) = \frac{d}{dt}[\theta(0)] = 0 \tag{21}$$

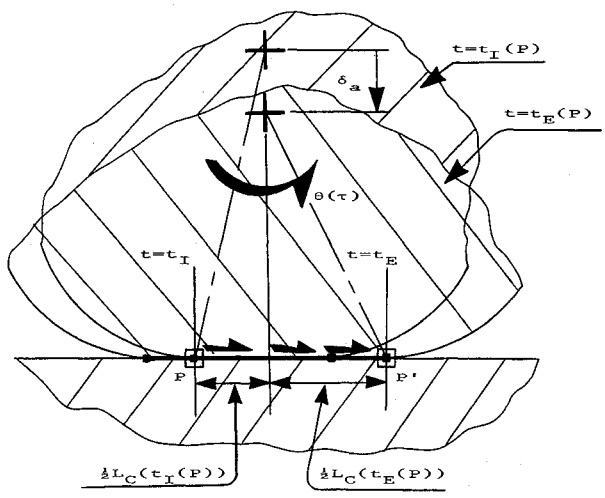

Fig. 5 Motion of contacted tire periphery points.

III. Solution

Overall, Eqs. (16), (17), and (19) are nonlinear ordinary differential equations. The nonlinearity arises from the force deflection characteristics of the tire, i.e., Eq. (15). For the current purposes, the solution is obtained by numerical integration, i.e., the Newmark Beta method.[7,9,10] Several response features will be sought. These include 1) the deflection, rotation, and velocity histories; 2) the net and pointwise growth of tire rotary KE; 3) the net and pointwise friction work history; and 4) the skid distance as a function of sink rate, friction coefficient, airplane velocity, etc.

To establish the pointwise friction work history, rotary KE growth, and skidding, we need to establish the contact residency time for each point on the tire periphery. Note the process of skidding ceases when

$$[R - \delta_a(t_T)]\frac{d}{dt}[\theta(t_R)] \equiv V_L(t_R) \tag{22}$$

such that t_R defines the time when pure rolling starts. For $t < t_R$, the points on the tire periphery undergo a mix of sliding and rolling. Throughout such times, the length of contact L_C is also undergoing changes. Because of the high internal pressure of typical aircraft tires (300 psi Shuttle), a good approximation of L_C is given by the expression[6]

$$L_C \sim \frac{F_N}{h_T P_I} \tag{23}$$

such that h_T is the width of the tire tread zone. Equation (23) has been compared to experimental data over a wide range of realistic pressures with good success.[6] Since the tire undergoes significant deformation during contact, the position of periphery points will be defined by the arc length position, i.e., S.

Based on the foregoing, when a given periphery point P with arc length position S_p initiates contact, its starting time is flagged as $t_I(P)$. Noting Fig. 5, this marks its upstream onset position, i.e., $0.5L_C[t_I(P)]$. At its exiting time $t_E(P)$, its downstream position is set by $0.5L_C[t_E(P)]$. Note its progress along the contact trajectory is defined by the periphery speed equal to $[R(0) - \delta_a(t)]\theta(t)$. In this context, to determine the pointwise residency time $t_R(P)$, we must solve the following nonlinear integral equation

$$\frac{1}{2}\{L_C[t_I(P)] + L_C[t_E(P)]\} = \int_{t_I(P)}^{t_E(P)} [R(0) - \delta_a(\tau)]\frac{d}{dt}[\theta(\tau)]\,d\tau \tag{24}$$

such that

$$t_R(P) = t_E(P) - t_I(P) \tag{25}$$

This can be achieved via the use of numerical quadrature. Recast numerically, Eq. (24) yields the expression[11]

$$\tfrac{1}{2}\{L_C(t_I) + L_C(t_I + n\Delta t_R)\} = \sum_{\ell=1}^{n} H_\ell \Delta t_R \,[R(0) - \delta_a(t_I + n\Delta t_R)]\frac{\mathrm{d}}{\mathrm{d}t}[\theta(t_I + n\Delta t_R)] \tag{26}$$

such that H_ℓ defines the quadrature weight. The solution is obtained by incrementing n until the right and left sides of Eq. (26) are equalized to within a preset tolerance. Note the Δt_R time increment must be very small: 10^{-4} s. This follows from the fact that the overall spinup time is usually 10^{-1} s or less.[2] Hence, typically, $\Delta t_R \ll 10^{-1}$ s.

Once $t_R(P)$ is known, the various pointwise histories can be determined. These include

1) Pointwise friction work:

$$W_{\text{slip}}(P) = \sum_{\ell} \int_{t_I^\ell}^{t_I^\ell + t_R^\ell} F_\mu V_{\text{slip}}\, \mathrm{d}t \tag{27}$$

2) Pointwise growth of tire rotary KE:

$$_R(\text{KE})_T|P = \sum_{\ell} \int_{t_I^\ell}^{t_I^\ell + t_R^\ell} F_\mu[R(0) - \delta_a]\frac{\mathrm{d}}{\mathrm{d}t}(\theta)\,\mathrm{d}t \tag{28}$$

3) Net pointwise residency time:

$$t_R = \sum_{\ell} t_R^\ell \tag{29}$$

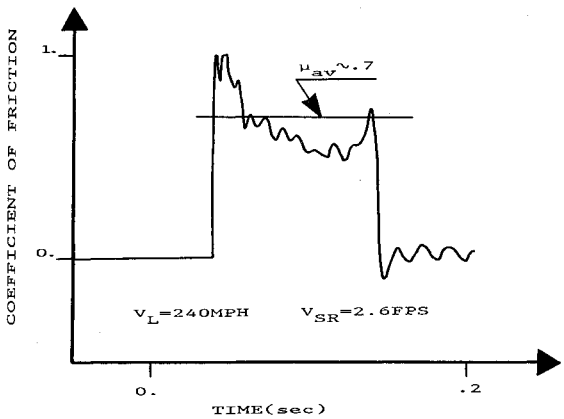

Fig. 6 Friction force rough runway: Kennedy Field.

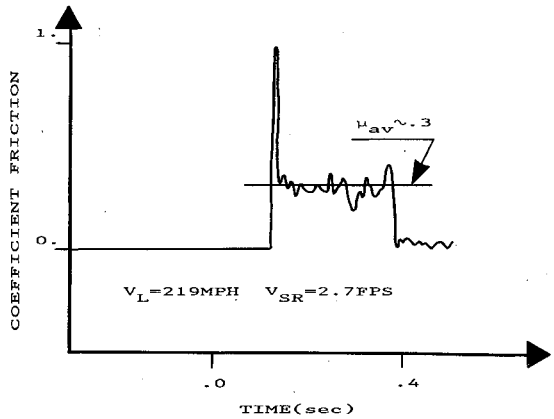

Fig. 7 Friction force smooth runway.

4) Net pointwise skid distance:

$$S_D(P) = \sum_{\ell} \int_{t_I^\ell}^{t_I^\ell + t_R^\ell} [R(0) - \delta_a]\frac{\mathrm{d}}{\mathrm{d}t}(\theta)\,\mathrm{d}t \tag{30}$$

5) Overall skid distance:

$$S_D(\text{total}) = \int_0^{t_R} [R(0) - \delta_a)]\frac{\mathrm{d}}{\mathrm{d}t}(\theta)\,\mathrm{d}t \tag{31}$$

In the above relations, the ℓ superscript and associated summations define situations in which a point may move into and out of contact during successive rolls.

IV. Case Study: Spinup of Shuttle Main Tires

As has been seen earlier, the model development requires a certain level of empiricism. This includes experimentally defined values of μ, $F_N - \delta_a$ behavior, J_T, M_a, C_T, $C_S(\delta_a)$, K_s, and P_I. Because of the short duration of spinup, the effects of C_T and C_S are negligible.

The coefficient of friction μ is a direct outgrowth of the mode of surface preparation of the runway. For instance, to

Table 1 Theoretical and experimental spinup times for rough and smooth runways

μ	V_L, knot	V_{SR}, ft/s	t_R(s) Experiment	t_R(s) Theory
0.3	240	2.7	0.26	0.241
0.7	219	2.6	0.108	0.101

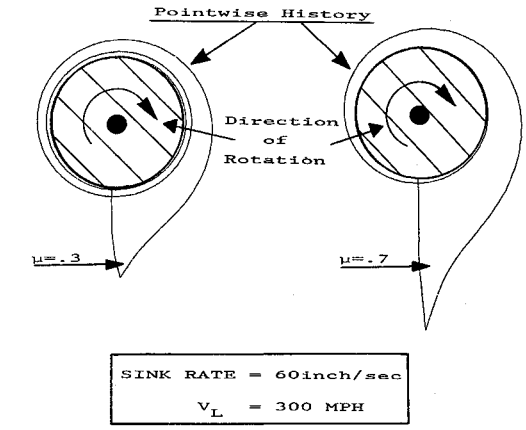

Fig. 8 Pointwise slip work history as a function of circumferential position: friction effects.

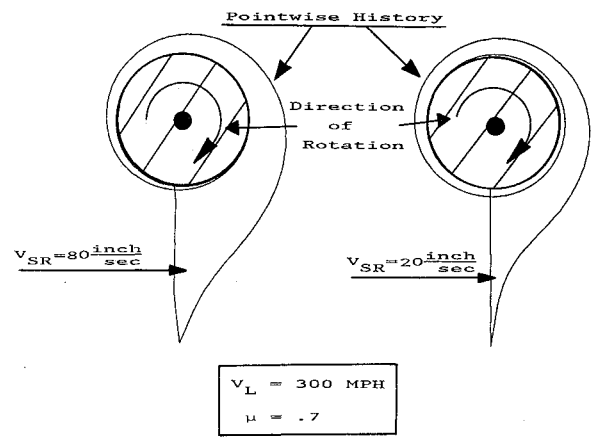

Fig. 9 Pointwise slip work history as a function of circumferential position: sink rate effects.

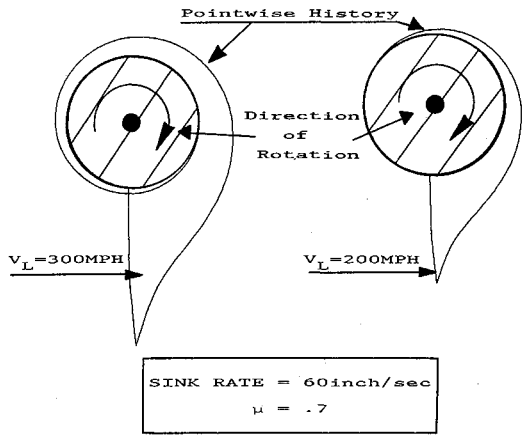

Fig. 10 Pointwise slip work history as a function of circumferential position: vehicle velocity effects.

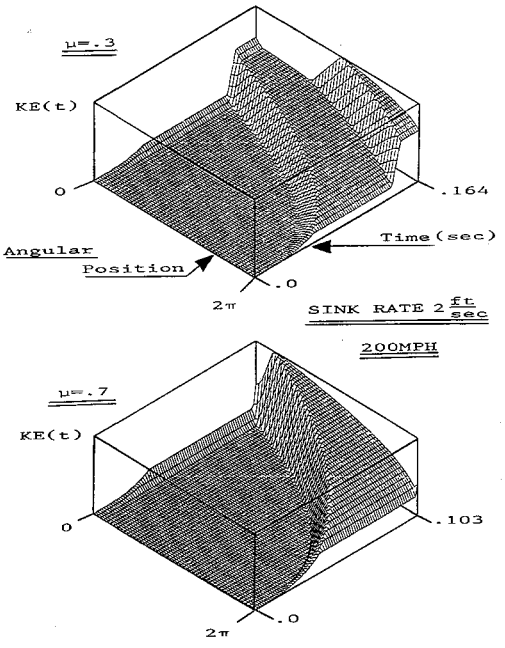

Fig. 11 Pointwise rotary energy input: sink rate 2 ft/s.

prevent hydroplaning, the initial rough coat of the NASA Kennedy landing field possesses a high coefficient of friction ($\mu \sim 0.7$). Figure 6 illustrates a typical friction drag force history generated during spinup on such a runway.[3] Based on a least squares type analysis,[12] a best μ fit can be estimated with reasonable statistical confidence limits. Such an analysis can be performed for a variety of runway surfaces, i.e., Fig. 7 illustrates a smoother, commercial-type surface.

To obtain the tire force deflection behavior (F_N/δ_a), a flat bed test[6] can be utilized. Figure 4 illustrates the effects of internal pressure on such behavior. As noted earlier, because of the Hertzian nature of contact,[6,7] the (F_N/δ_a) behavior is essentially of the hardening type. To complete the data for the Shuttle tire,[8] J_T = 194 in.-lb/s^2; gM_a = 196 lb; $K_T \sim$ 18,670 lb/in.; R = 22.43 in.; and $P_I \epsilon$ (290, 340 psia).

Next, to benchmark the adequacy of the model, we shall consider evaluating the spinup time for two experimental test cases involving smooth and rough runaways. Table 1 presents the theoretical-experimental comparisons. As can be seen, excellent correlation is achieved.

In this context, we shall employ the model to establish the range of influence of such factors as sink rate, μ, and V_L. Figures 8–10 illustrate the pointwise friction work history, As can be seen, the maximum pointwise rate of slip work occurs at the early stages of skidding. This is a direct result of the

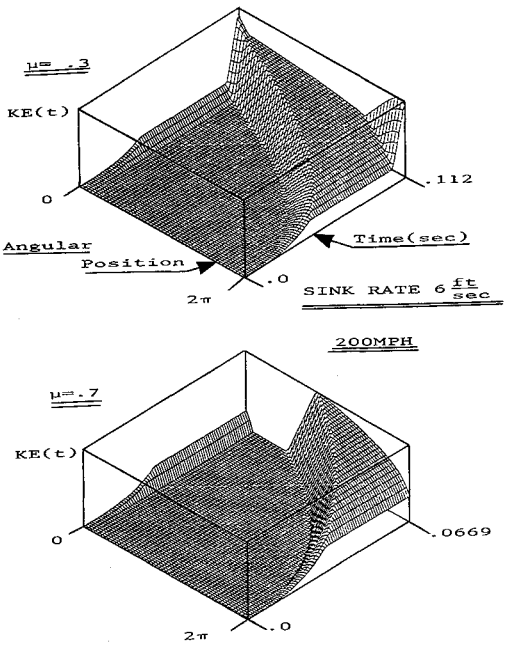

Fig. 12 Pointwise rotary energy input: sink rate 6 ft/s.

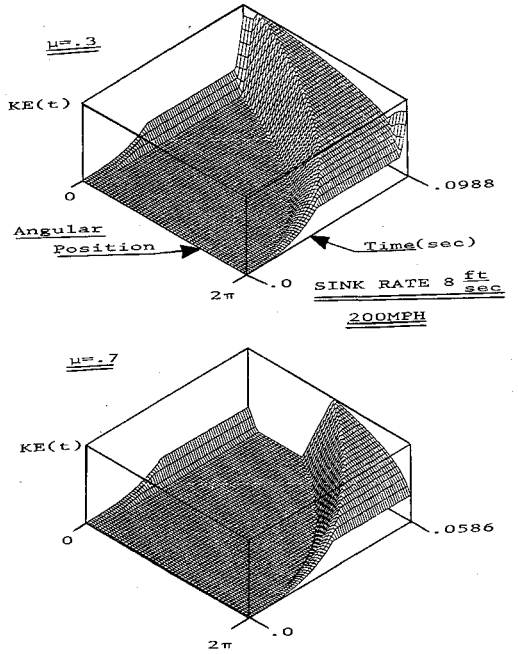

Fig. 13 Pointwise rotary energy input: sink rate 8 ft/s.

initially high slip velocities. Note that the wear patterns generated during actual spinup coincide with the slip work rate profiles.

Noting the parametric trends depicted in Figs. 8–10, it follows that the slip work rate is modified by parametric variations in sink rate (V_{SR}), μ, and V_L are raised. This leads to shorter spinup times and concomitantly shortened runway skid zones and wear patches on the tire. In a similar context, Figs. 11–13 illustrate the pointwise growth of rotary KE. Similar to the slip work rate, the spinup process is greatly intensified with increases in V_{SR}, μ, and V_L.

Perhaps the easiest way to illustrate the effects of parametric variations is to consider the number of tire revolutions and the spinup time during the skidding phase of spinup. Such trends are depicted in Figs. 14 and 15. As can be seen, for smooth runways ($\mu \sim 0.2$) and low sink rate landings ($V_{SR} \sim 2$ ft/s), the tire undergoes several revolutions before reaching

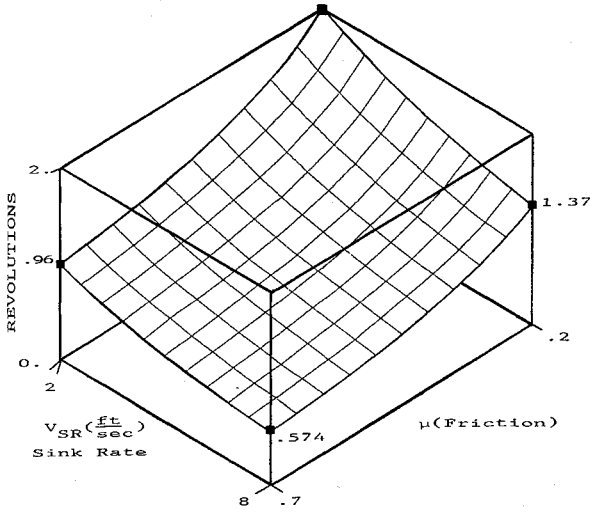

Fig. 14 Parametric effects of sink rate and friction coefficient on skidding distance: number of tire rotations.

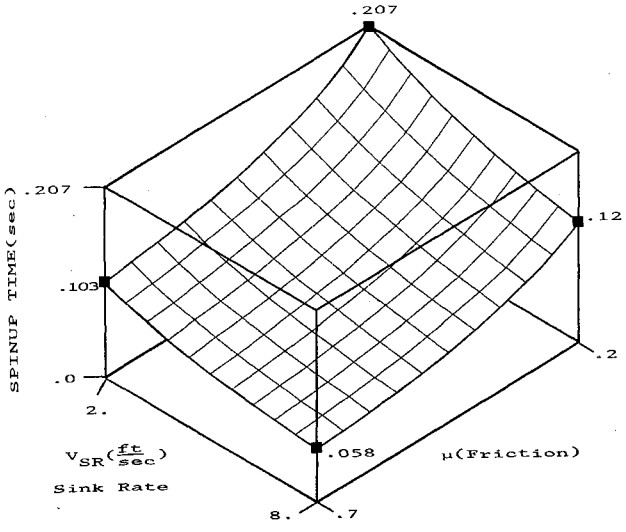

Fig. 15 Parametric effects of sink rate and friction coefficient on skidding distance: spinup time.

rolling speed. This obviously yields low wear rate intensities since the process is spread over greater periphery dimensions. In contrast, for rough runways ($\mu \sim 0.7$) and high sink landings ($V_{SR} > 2$ ft/s), very short periphery dimensions are involved: a fractional part of a revolution.

V. Conclusions

Given its reasonable simplicity, the tire spinup model developed in the preceding sections yields a good assessment of the various factors impinging the overall process. This includes gauging the effects of sink rate, runway frictional characteristics, vehicle landing speed, stiffness and inertial properties of the tire-brake-rim-axle system, as well as suspension system tuning.

Since the model yielded spinup times and skid distances which correlated well with experiment, it follows that it provides a good balance of energy flows, i.e., into rotary KE and slip work. As noted earlier, the slip work is itself apportioned into two basic modes, namely heat buildup and high rate wear/machining. In a followup study, the model developed herein will be employed to establish the flash surface thermal fields and potential wear rates.

Acknowledgment

The first author acknowledges the helpful discussions with John Tanner and colleagues of the NASA Langley landings branch.

References

[1]Currey, N. S., *Landing Gear: Design Handbook,* 1st ed., Lockheed Georgia Co., Marietta, GA, Jan. 1983.

[2]Captain, K. M., Stokes, V. K., and Edwards, J. H., "Friction and Wear Test for Aircraft Tires," Aeronautical Systems Div., Air Force System Command, Wright Patterson Air Force Base, OH, TR-ASR-TR-72-85, Nov.1972.

[3]Tanner, J. A., Drchet, R. C., Stubbs, S. M., and Smith, E. G., "Tire Temperatures During Antiskid Braking and Cornering Over Dry Runway," NASA TP-2009, May 1982.

[4]Dougherty, R. H., and Stubbs, S. M., "Spinup Studies of the Space Shuttle Orbiter Main Gear Tire," NASA SAE 881360, Aerospace Technical Conference, Anaheim, CA, Oct. 1988.

[5]Chung, T. J., *Continuum Mechanics,* Prentice-Hall, Englewood Cliffs, NJ, 1988.

[6]Clark, S., *Mechanics of Pneumatic Tires,* Dept. of Transportation, National Highway Traffic Safety Administration, U. S. Government Printing Office, 1980.

[7]Padovan, J., Kennedy, R., and Nakajima, Y., "Finite Element Analysis of Steady and Transiently Moving/Rolling Nonlinear Viscoelastic Structure: Parts 1, 2, 3," *Computers and Structures,* Vol. 27, 1987, pp. 249-286.

[8]Moravec, B. A., Trikha, A. K., Scholtz, R. C., and Jurczak, J. T., "Advanced Tire Development for Hypervelocity Vehicles," WRDC-TR-89-3033, May 1989.

[9]Padovan, J., and Kazempour, A., "Multibody Instantly Centered Moving Lagrangian Observer Schemes," *Computers and Structures,* Vol. 32, 1989, pp. 93-111.

[10]Hughes, T. J. R., *The Finite Element Method,* Prentice-Hall, Englewood Cliffs, NJ, 1987.

[11]Baker, C. T. H., *The Numerical Treatment of Integral Equations,* Clarendon Press, Oxford, 1977.

[12]Bevington, P. R., *Data Reduction and Error Analysis for the Physical Sciences,* McGraw-Hill, New York, 1969.